

Monte Carlo Study of Thermal Transport of Frequency and Direction Dependent Reflecting Boundaries in High Kn Systems

N.A. Roberts

Department of Mechanical Engineering
Vanderbilt University
Nashville, TN 37235
Email: nicholas.a.roberts@vanderbilt.edu

D.G. Walker

Department of Mechanical Engineering
Vanderbilt University
Nashville, TN 37235
Email: greg.walker@vanderbilt.edu

Abstract—The effective thermal conductivity of non-continuum wires with rough boundaries was investigated theoretically. The boundaries were designed to reflect phonons differently depending on the phonon frequency or the angle of incidence. Devices with these properties could be useful in thermal management problems on the nanoscale and microscale. In the first study the scattering was dependent on the frequency of the phonons where lower frequency phonons reflected diffusely while higher frequency phonons reflected specularly. In the directional study a parameter p , which is a function of the x-component of direction and the phonon frequency, was used to account for the degree of specularity. This work studied the effects of varying the cutoff frequency and the device size, including length and cross section. A one-dimensional Monte Carlo simulation of phonon transport was used to investigate the thermal conductivity of a device with adiabatic boundaries. This difference in scattering emerges from the geometry and magnitude of rough surfaces where the roughness is of the order of the dominant phonon wavelength.

I. INTRODUCTION

Thermal rectification is a phenomenon where transport through a material is dependent on the direction, and though its observations in solids have been rare, rectifying behavior could have wide spread applications. Records of rectification date back as early as 1935 when Starr [1] found that copper/cuprous oxide systems showed thermal as well as electrical rectification. Walker [2] presented evidence and several candidate theoretical models for rectification behavior. Most models suggest that rectification could be exploited with our improved ability to manipulate materials at the nanoscale. In 2002 Terraneo et al. [3] demonstrated theoretical rectification behavior using a nonlinear one-dimensional chain of atoms between two thermostats at different temperatures with a constant temperature difference where they were able to change the chain from a normal conductor to a nearly perfect insulator. In a similar study in 2004, Baowen et al. [4] simulated a nonlinear lattice and calculated a difference in conduction between the two directions to be 100 times that of [3]. In 2006 Chang et al. [5] suggested that solitons were responsible for rectification and showed that greater conduction resulted in the direction of decreasing mass density in an engineered material having non-uniform mass distribution along the carbon and boron nitride nanotubes.

Through phonon transport simulations we provide theoretical evidence of the existence of thermal rectifying behavior in devices with nanostructured boundaries. Many studies, both experimental and theoretical, have been performed and reported for thermal transport in low-dimensional solids including thin films and nanowires [6–10]. The theoretical studies typically seen are based on the Boltzmann Transport Equation (BTE) or molecular dynamics simulations. These methods have been very effective in explaining thermal transport, specifically in nanoscaled structures. The BTE has been very useful because it is possible to achieve a closed form analytic solution when introducing numerous assumptions [6], though results can differ significantly from experimental results [11]. Monte Carlo simulations have also been very

NOMENCLATURE

a	lattice constant (m)
b	polarization (acoustic phonon branch)
d	degree of specularity
$D(\omega)$	density of states (m^{-3}s)
$F(\omega)$	normalized density function
$\mathcal{F}_{12}, \mathcal{F}_{21}$	exchange factors
k, k_x	total and x-component wave vector (m^{-1})
l	device length (m)
$\langle n \rangle$	phonon occupation number
N	number of phonons
p	probability of specular reflection
R, R_1, R_2	random numbers
t	height of device roughness
T	temperature (K)
V_g	phonon group velocity (ms^{-1})
w	device width (m)
α	aspect ratio (l/w)
η	characteristic surface roughness (m)
ω	phonon frequency (Hz)
ω_{cutoff}	cutoff frequency (Hz)
ψ	azimuthal angle (rad)
θ	polar angle (rad)

effective where both the transverse and longitudinal acoustic phonon polarizations and phonon dispersions are considered [7]. Monte Carlo simulations have been used by Chen et al. [8] to calculate the thermal conductivity of individual silicon nanowires of different sizes over a wide range of temperatures and the results show reasonable agreement with experimental data [9, 10]. In these studies the surfaces were considered flat and the reflection from the surface was determined by a fixed parameter d , which is the degree of specularity. In 2006 Saha et al. [11] conducted a Monte Carlo simulation of phonon backscattering in a nanowire with V-shaped surface roughness to explain the difference in measured and calculated thermal conductivities in silicon nanowires. Saha's work shows that phonon backscattering (partially diffuse and partially specular reflections) can indeed produce the reduced calculated thermal conductivity which is caused by the nanometer scale surface roughness present in the samples during the experimental studies [11]. In the present work we have used Saha's hypothesis to construct a device in which the surface roughness is dependent on the direction the phonon is traveling. This difference in surface roughness means the parameter that determines the type of reflection (specular or diffuse) is a function of the phonon's frequency and direction. To create this we have used boundaries that appear to be smooth to phonons traveling in one direction while appearing to be rough (characteristic roughness of the order of the phonon wavelength) to phonons traveling in the opposite direction. This surface can be realized as a sawtooth (an asymmetric version of the V-shaped surface from ref. [11]) as seen in Figure 1 where each of the two surfaces have different roughnesses. The dimensions of the sawtooth shape needs to be of the order or less than the phonon wavelength to result in a directional dependence for reflections. In our actual simulations the boundaries are flat, and the structured features are modeled by introducing asymmetric reflection at the surface.

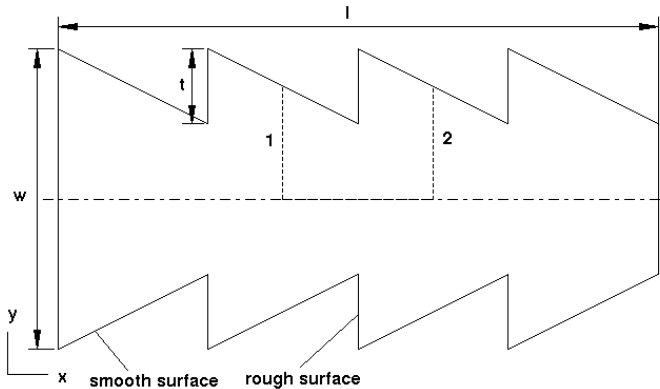


Fig. 1. Diagram of the simulated geometry where one surface is smooth ($\eta = 0$) and the other surface is rough ($\eta > 0$). In the actual simulation the boundaries are flat. The dotted line represents the system used in the MONT2D simulations.

Phonons striking the smooth surface will reflect specularly, and those that strike the rough surface will reflect either spec-

ularly or diffusely depending on the roughness of that surface and the wavelength of the phonon. Due to the asymmetry of these boundaries, it is possible to obtain a self-biasing device meaning the device would prefer thermal transport in one direction over the other. This device behaves as a thermal rectifier.

II. SIMULATION METHOD

In this work we have used a Monte Carlo (MC) method to simulate the phonon transport described in [7]. The number of phonons (1,000,000) is initially prescribed and their polarizations and frequencies are obtained based on an initial temperature assuming equilibrium. The location of each phonon is determined from a uniform distribution in all three dimensions. The individual components of momentum are calculated using,

$$k_x = k \sin \theta \cos \psi \quad (1)$$

$$k_y = k \sin \theta \sin \psi \quad (2)$$

$$k_z = k \cos \theta \quad (3)$$

where k is the total isotropic momentum. The directions $\cos \theta = 2R_1 - 1$ and $\psi = 2\pi R_2$ which are the polar and azimuthal angles, are chosen from a uniformly distributed random number R_1 and R_2 , which ranges from zero to one. In this work we assume an analytic dispersion with a maximum transverse and longitudinal frequency of 4.5×10^{12} Hz and 1.23×10^{13} Hz respectively which approximates the values for silicon. The full details of the simulation can be found in reference [7]. A frequency range from zero to the maximum frequency of the longitudinal acoustic branch is divided into 1000 equally spaced discrete values. Optical phonon modes are neglected in this study because of their minimal contribution to the thermal transport due to their small group velocity [12]. This study is strictly within the ballistic transport regime therefore we are not considering three-phonon or impurity scattering in order to isolate the effects of the boundaries alone.

After the phonons have been initialized they are allowed to drift linearly based on their individual momenta for a prescribed time step of 5 ps for a total of 50 ns. If a phonon crosses a boundary during the drift phase it is backed up to the first boundary it strikes and is reflected. The reflection of the phonon is dependent on the sign of the x-component of momentum (k_x) and it's frequency. If a phonon has a positive k_x it will always reflect specularly because it will strike the "smooth" surface, but if a phonon has a negative k_x then a scattering parameter p will be calculated, which is given by

$$p(\omega) = \exp \left[-\frac{64\pi^5 \eta^2 \omega^2}{V_g^2} \right], \quad (4)$$

where V_g is the group velocity and η is the characteristic roughness of the surface [13]. A random number (R) is then generated and compared to p , if $p > R$ the phonon is reflected specularly, otherwise it is reflected diffusely. For the diffuse reflection the individual components of momentum are recalculated with the same total momentum and frequency in order to conserve energy. The phonon is then allowed to drift

for the remainder of the time step. After each time step the energy, number of phonons and average temperatures of each of the 100 cells is calculated.

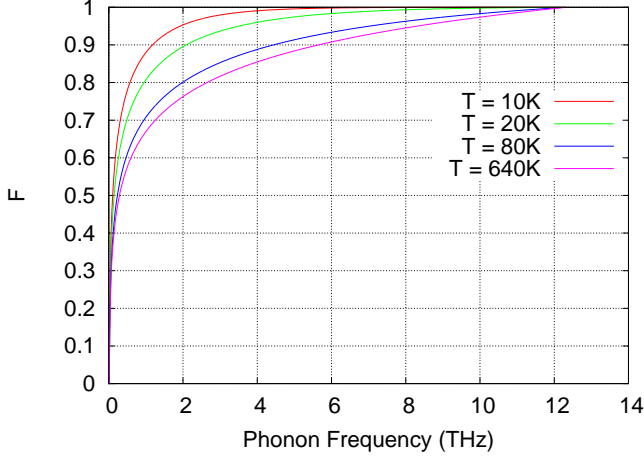


Fig. 2. Normalized phonon number density as a function of phonon frequency at at various temperatures

In this work we studied systems with cross sections of $100 \text{ nm} \times 100 \text{ nm}$, $500 \text{ nm} \times 500 \text{ nm}$ and $1000 \text{ nm} \times 1000 \text{ nm}$ with lengths of 100 nm , 500 nm and 1000 nm . We also varied the roughness of the surface seen by the left-moving phonons with values of $\eta = 0$ to $1 \times 10^{-9} \text{ m}$. These roughnesses directly impact the probability of a specular reflection p . As the roughness increases, the probability of reflecting specularly decreases.

A cutoff frequency can be obtained by setting $p = 0.5$ and then calculating the frequency as a function of surface roughness as in equation 4. This cutoff frequency is the average frequency for which frequencies less than it will reflect specularly and frequencies greater than it will reflect diffusely. The normalized density function, which is seen in Figure 2 for various temperatures, is the fraction of phonons below a particular phonon frequency. This distribution shows that below a specified frequency there is a higher density of phonons for lower temperatures. With knowledge of the average cutoff frequency along with the normalized density function at a specific temperature one can approximate the level of self-biasing of the device. The normalized density function (F_ω) is given by,

$$F(\omega) = \sum_b \frac{\int_0^\omega \langle n \rangle D(\omega) d\omega}{\int_0^{\omega_{\max,b}} \langle n \rangle D(\omega) d\omega}, \quad (5)$$

where $\langle n \rangle$ is the Bose-Einstein distribution [12], $D(\omega)$ is the 3-D density of states given by,

$$D(\omega) = \frac{k^2}{2\pi^2 V_g}, \quad (6)$$

where k is given by,

$$k = \frac{\arccos\left(1 - \frac{2\omega^2}{\omega_{\max,b}^2}\right)}{a}. \quad (7)$$

Here b is the branch (LA or TA) and a is the lattice constant.

III. SIMULATION RESULTS

The results of our simulations show that with a roughness on the order of picometers on one side of the sawtooth we can achieve a self-biasing device. The level of self-biasing is related to the roughness so that an increased roughness leads to increased biasing until the surface has a characteristic roughness of around an angstrom at which point roughly all phonons traveling in the negative x -direction will reflect diffusely. At higher temperatures the influence of p will be lower than for lower temperatures because the average frequency of phonons at higher temperatures is larger. Smaller wavelength phonons will scatter more diffusely resulting in more self-biasing. The temperature distributions for a low temperature (10 K) (fewer high frequency phonons) and a high temperature (640 K) (more high frequency phonons) for a large and small aspect ratio (α) are shown in Figure 3. In this figure we see that the temperature distribution is a strong function of the surface roughness, the aspect ratio of the device and the initial equilibrium temperature. In these cases the boundaries create a non-equilibrium temperature distribution because they do not allow the phonons to interact freely and exchange energy and momentum and thus result in a temperature gradient with zero net flux. For the calculation of the temperature within each cell, local thermodynamic equilibrium is assumed and is found based on the cell's phonon energies. Local thermodynamic equilibrium is assumed to be valid because the phonons within each cell are allowed to interact relatively freely without a large impact from the boundaries.

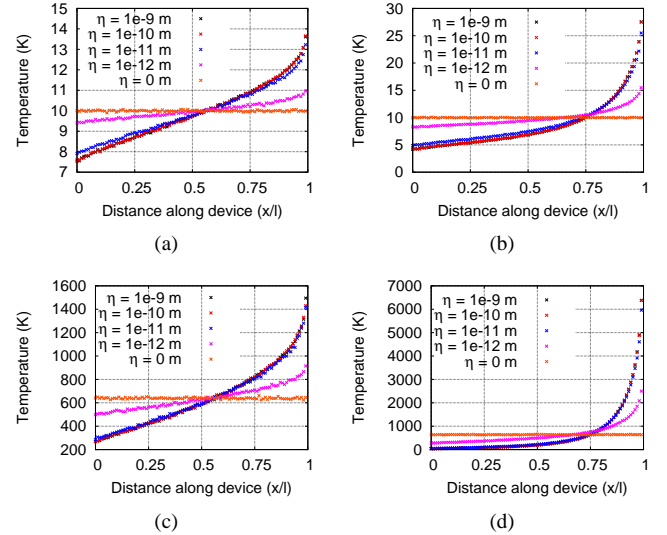


Fig. 3. Temperature distribution at 10K and 640K for different surface roughnesses and aspect ratios. (a) 10K with $\alpha = 1$. (b) 10K with $\alpha = 10$. (c) 640K with $\alpha = 1$. (d) 640K with $\alpha = 10$.

The amount of self-biasing predicted from the simulations can be seen in Figure 4 where the difference in the temperature of the right and left boundaries is shown as a function of the surface roughness at 10K for various aspect ratios.

As the surface roughness is increased the difference in the temperatures at the left and right sides (bias) becomes greater. This occurs because more phonons with negative values of k_x are being reflected diffusely, therefore there is an equal probability that they will return to the right side. Phonons traveling in the positive x-direction will reflect specularly and continue toward the right boundary. As a result phonons will tend to collect at the right boundary. A large change in the temperature difference is seen when the roughness goes from $\eta = 1 \times 10^{-12}$ m to $\eta = 1 \times 10^{-11}$ m. This occurs because the transition to the smoother surface results in a raising of the cutoff frequency to a level where fewer phonons exist (8×10^{12} Hz). For larger roughnesses the amount of phonons that is eligible to reflect diffusely does not increase significantly, so the temperature difference does not increase as rapidly. The temperature difference for $\eta = 0$ m was 0 with some statistical uncertainty ($\pm 2.5\%$), which is expected, when no diffuse reflections occur.

Figure 5 shows the normalized temperature difference at a fixed surface roughness of $\eta = 5 \times 10^{-12}$ m for various temperatures as a function of the aspect ratio (larger aspect ratio represents longer thinner wires). The normalized temperature difference increases with aspect ratio because the reflecting boundaries dominate the transport. As the temperature increases, more high frequency phonons are present, which causes a greater percentage of those with a negative x-component of momentum to scatter diffusely for a fixed surface roughness. This can also be deduced from Figure 2 where it is shown that there are a greater percentage of higher frequency phonons at higher temperatures. At a fixed cutoff frequency, a greater percentage of phonons will be reflected diffusely at higher temperatures resulting in the greater normalized temperature difference. Figure 5 agrees with intuition because if one were to either make the distance between the asymmetric boundaries smaller or make the device longer we would expect to see greater interaction with the boundaries which would enhance the self-biasing effect and result in a greater temperature difference between the right and left sides of the device.

This simplified model demonstrates the possibility of achieving a thermally self-biasing device, which lends credence to the idea of designing a device for thermal rectification. Upon initial inspection, the device appears to operate like a Maxwell's demon, which would violate the second law of thermodynamics if in equilibrium. For this reason, there is understandable debate over whether we have devised a non-physical scenario or if the system is not in equilibrium. Nevertheless, thermal rectification is seen in devices that have some asymmetry associated with the geometry. For example, natural convection in an enclosure where the heat transfer is in the vertical direction exhibits a rectification effect. When the bottom is heated, buoyancy-induced flow results in a larger heat transfer coefficient than when the top surface is heated. In the latter, the heat transfer is by conduction through a gas only, which is generally small compared to convection in that same gas. In the natural convective example, gravity breaks

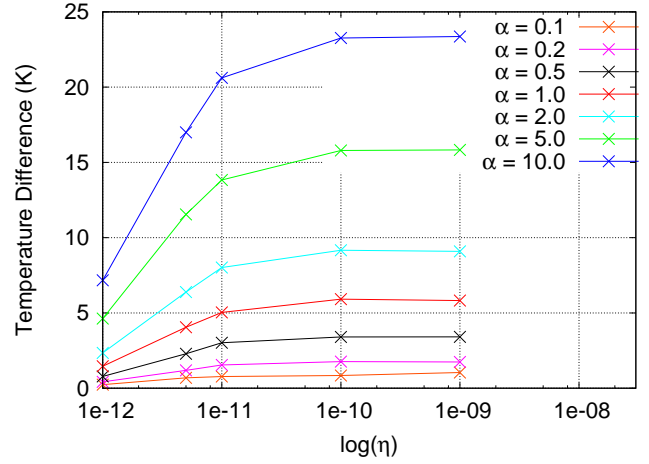


Fig. 4. Temperature difference at 10K for different surface roughnesses and aspect ratios

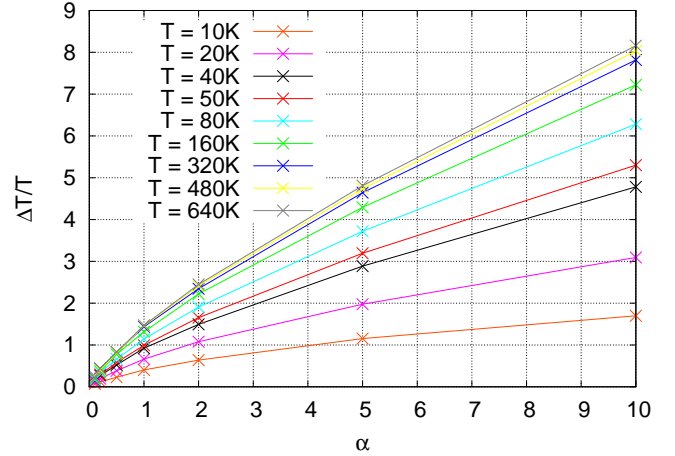


Fig. 5. Normalized temperature difference for $\eta = 5 \times 10^{-12}$ m versus the device aspect ratio in a temperature range from 0 to 640K

the symmetry of the system. In the foregoing example, the selective boundary breaks the symmetry.

An analogy to this rectification effect can also be drawn with that in a pn -junction where the drift current and diffusion current are non-zero, yet the net current is zero. The drift current is a result of motion of charge carriers under an applied electric field. The diffusion current is a result of the diffusion of particles from an area of high concentration to an area of low concentration. In a pn -junction, two materials of differing charge carrier concentrations are brought into contact which allows the carriers in the material with a higher concentration to diffuse into the other material. Because of this diffusion process a current is then established as a result of no external forces which is a non-physical effect. To obtain a zero net current there must be an equal and opposite drift current which implies that a non-zero internal electric field develops at the junction. In the current work it can be argued that a similar effect is occurring. The boundaries create a non-uniform phonon distribution due to the directional and frequency dependence

of the phonon reflections. This is analogous to the diffusion current in the pn -junction. Because the device is insulated from external forces there must be an equal and opposite flux to obtain no net flux in the device. In this case a non-zero temperature gradient exists which is analogous to the non-zero internal electric field in the pn -junction. This can be seen by examining the phonon and temperature distribution as a function of time within the device where, as mentioned previously, the higher frequency phonons collect near the right boundary when the characteristic surface roughness seen by the phonons moving in the negative x -direction is greater than zero.

In the Monte Carlo model, the boundary was assumed flat because the roughness is typically much smaller than the device dimensions. Moreover, the roughness is comparable to the phonon wavelength. The fact that the boundary has a geometric feature that interacts with the phonons at the boundary is included by fabricating selectively diffuse or specular reflections. A sawtooth structure, which appears different from each direction, is used to motivate this type of boundary. We also note that a sawtooth structure does not produce rectification if the phonon wavelength is smaller than the height of the sawtooth. In this case the transport can be predicted by a radiation exchange factor analysis. The tool MONT2D [14] was used to predict the exchange factors for the enclosure shown in Figure 1. The reflectivity of the sawtooth surfaces was unity but the nature of the reflection was changed between purely diffuse and purely specular, resulting in four possible configurations. In addition to the surface properties, the height of the sawtooth relative to the device size was also varied. In no case was the exchange factor \mathcal{F}_{12} found to be different than \mathcal{F}_{21} . Table I summarizes the results for two different sawtooth sizes. These results imply that the fabricated device boundaries must not only be asymmetric to obtain a directional dependence, but they must also differ in surface roughness to result in a frequency dependence and rectification behavior. To fabricate a device of this type would require great control of the geometry and quality of the boundaries. Various fabrication and characterization techniques could be used for this device [9, 10, 15–18] although with current technology, these ideal boundaries could be extremely difficult to create.

IV. CONCLUSION

In the present work, a Monte Carlo simulation was used to predict self-biasing effects originating from asymmetric boundaries of a wire. In the limiting case, phonons striking the boundary from a preferred direction reflect diffusely. Phonons striking the boundary from the other direction reflect specularly. This asymmetry produces a bias in the device such that the number, energy and resulting temperature are higher on the preferred side where the phonons collect. The distribution is non-equilibrium in nature, so the temperature represents the average temperature of the phonons, not necessarily the equilibrium temperature. The purely diffuse scattering phonons from the preferred side represents a limiting case and maximum rectification effect. For cases where the

TABLE I
RADIATION EXCHANGE FACTORS FOR CONFIGURATION SHOWN IN FIGURE 1. THE DIFFERENCE REPRESENTS THE AMOUNT OF RECTIFICATION. THE THREE SURFACES OF THE SAWTOOTH STRUCTURE ARE SPECULAR (S) OR DIFFUSE (D). THE ERROR ASSOCIATED WITH TOOTH HEIGHT $t = 1.8$ IS 6.06×10^{-4} , AND THAT ASSOCIATED WITH $t = 0.2$ IS 9.83×10^{-4} . THEREFORE, NO CONFIGURATION EXHIBITS RECTIFICATION.

t	surface	\mathcal{F}_{12}	\mathcal{F}_{21}
1.8	SSS	0.09675	0.09609
	DDD	0.09550	0.09551
	DSD	0.09656	0.09880
	SDS	0.09751	0.09591
0.2	SSS	0.82446	0.82547
	DDD	0.65363	0.65481
	DSD	0.65836	0.65790
	SDS	0.83013	0.83205

reflection is related to the roughness, rectification is reduced, and an unbiased device is recovered for symmetric boundaries.

The Monte Carlo results are predicated on the assumption that surface features are of the order of phonon wavelengths and that an asymmetric surface can be designed and built. For simulations involving large features compared to the phonon wavelengths, no rectification is seen. Therefore, rectification is only possible with nanostructured materials. Whether the device can actually be built is under investigation.

These findings suggest that new materials can be used to provide advanced passive thermal control of localized transport. In the present context, we have used the amount of self-biasing as an indication of how strong the rectification might be. However, once the device is connected to thermalizing reservoirs, the frequency content at each end will change. In the limiting case of pure diffuse reflection of phonons from the preferred direction, the selection is not frequency dependent, so the bias is due to the number of phonons and not the frequency content of those phonons. Therefore, thermalizing boundaries will not change the frequency content of the collection of phonons. Therefore, in a biased device, applied temperature gradient, we expect heat transfer that is proportional to the self bias added to the applied bias.

REFERENCES

- [1] C. Starr, “The copper oxide rectifier”, *Physics (Journal of Applied Physics)*, vol. 7, pp. 15–19, Jan. 1935.
- [2] D. G. Walker, “Thermal rectification mechanisms including noncontinuum effects”, in *proceedings of the Joint ASME-ISHMT Heat Transfer Conference*, IIT Guwahati, India, Jan. 2006.
- [3] M. Terraneo, M. Peyrard, and G. Casati, “Controlling the energy flow in non-linear lattices: A model for a thermal rectifier”, *Physical Review Letters*, vol. 88, no. 9, pp. 4302.1–4302.4, Mar. 2002.
- [4] L. Baowen, W. Lei, and C. Giulio, “Thermal diode: Rectification of heat flux”, *Physical Review Letters*, vol. 93, no. 18, Oct. 2004.
- [5] C. W. Chang, D. Okawa, A. Majumdar, and A. Zettl, “Solid-state thermal rectifier”, *Science*, vol. 314, pp. 1121–1124, Nov. 2006.

- [6] M. G. Holland, "Analysis of lattice thermal conductivity", *Physical Review*, vol. 132, no. 6, pp. 2461–2471, Dec. 1963.
- [7] S. Mazumder and A. Majumdar, "Monte carlo study of phonon transport in solid thin films including dispersion and polarization", *Journal of Heat Transfer*, vol. 123, no. 4, pp. 749–759, June 2001.
- [8] Y. Chen, D. Li, J. Lukes, and A. Majumdar, "Monte carlo simulation of silicon nanowire thermal conductivity", *Journal of Heat Transfer*, vol. 127, pp. 1129–1137, 2005.
- [9] D. Y. Li, Y. Wu, P. Kim, L. Shi, P. D. Yang, and A. Majumdar, "Thermal conductivity of individual silicon nanowires", *Applied Physics Letters*, vol. 83, no. 14, pp. 2934–2936, Oct. 2003.
- [10] D. Y. Li, Y. Wu, R. Fan, P. D. Yang, and A. Majumdar, "Thermal conductivity of Si/SiGe superlattice nanowires", *Applied Physics Letters*, vol. 83, no. 15, pp. 3186–3188, Oct. 2003.
- [11] S. Saha, L. Shi, and R. Prasher, "Monte carlo simulation of phonon backscattering in a nanowire", in *Proceedings of the ASME International Mechanical Engineering Congress and Exposition*, Chicago, IL, Nov. 2006.
- [12] C. Kittel, *Introduction to Solid State Physics*, Wiley, New York, 6th edition, 1986.
- [13] J. M. Ziman, *Electrons and Phonons*, Oxford University Press, London, 1960.
- [14] "mont2d <http://www.colostate.edu/pburns/monte/code.html>".
- [15] Y. Wu, R. Fan, and P. Yang, "Block-by-block growth of single-crystalline Si/SiGe superlattice nanowires", *Nano Letters*, vol. 2, no. 2, pp. 83–86, 2002.
- [16] A. R. Abramson, W. C. Kim, S. T. Huxtable, H. Yan, Y. Wu, A. Majumdar, C.-L. Tien, and P. Yang, "Fabrication and characterization of a nanowire/polymer-based nanocomposite for a prototype thermoelectric device", *Journal of Microelectromechanical Systems*, vol. 13, no. 3, pp. 505–513, June 2004.
- [17] P. Kim, L. Shi, A. Majumdar, and P. L. McEuen, "Thermal transport measurements of individual multiwalled nanotubes", *Physical Review Letters*, vol. 87, no. 21, pp. 215502–1–215502–2, Nov. 2001.
- [18] L. Shi, D. Li, C. Yu, W. Jang, D. Kim, Z. Yao, P. Kim, and A. Majumdar, "Measuring thermal and thermoelectric properties of one-dimensional nanostructures using a microfabricated device", *Journal of Heat Transfer*, vol. 125, pp. 881–888, 2003.